ACS APPLIED MATERIALS & INTERFACES

Research Article

www.acsami.org

Facile and Selective Synthesis of Oligothiophene-Based Sensitizer Isomers: An Approach toward Efficient Dye-Sensitized Solar Cells

Quanyou Feng, Qian Zhang, Xuefeng Lu, Hong Wang, Gang Zhou,* and Zhong-Sheng Wang*

Laboratory of Advanced Materials & Department of Chemistry, Fudan University, 2005 Songhu Road, Shanghai 200438, P. R. China

Supporting Information

ABSTRACT: Two sets of isomeric organic dyes with *n*-hexyl (**DH** and **AH**) or 2-ethylhexyl (**DEH** and **AEH**) groups substituted at the spacer part have been designed and straightforwardly synthesized via a facile and selective synthetic route. The structure difference between the isomers stands at the position of the incorporated alkyl chains which are introduced into the terthiophene spacer close to the donor (**D**) or anchor (**A**) side. The relationship between the isomeric structures and the optoelectronic properties are systematically investigated. It is found that, in the **D** series dyes, the alkyl group is much closer to the aromatic donor moiety, which brings about strong steric hindrance and therefore causes a remarkable twist in the molecular skeleton. In contrast, a more planar chemical structure and more effective π-conjugation are realized in the **A** series dye isomers. Consequently, the **A** series isomeric dyes demonstrate bathochromically shifted absorption bands, resulting in the improved light-harvesting capability and enhanced photo-generated current. However, the **D** series isomeric dyes with more twisted molecular skeleton have suppressed the intermolecular interactions and retarded the charge recombination more efficiently, which induces higher open-circuit photovoltage. Combining the two effects on the performance of the fabricated dye-sensitized solar cells (DSSC), the influence from the short-circuit photocurrent plays a more significant role on the power conversion efficiency (η). As a result, isomer **AEH**-based DSSC with quasi-solid-state electrolyte displays the highest η of 7.10% which remained at 98% of the initial value after continuous light soaking for 1000 h. Promisingly, a η of 8.66% has been achieved for **AEH**-based DSSC with liquid electrolyte containing Co(II)/(III) redox couple. This work presents the crucial issue of molecular engineering and paves a way to design organic sensitizers for highly efficient and stable DSSCs.

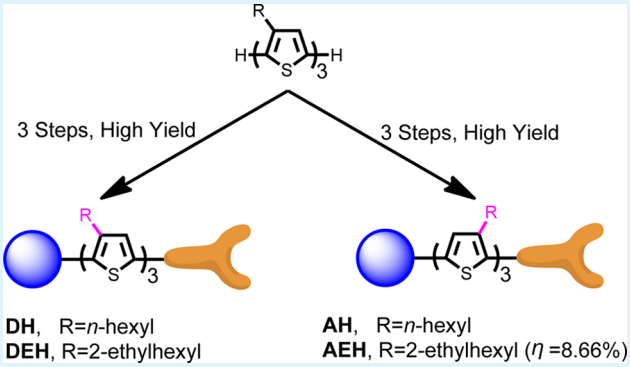

KEYWORDS: *charge recombination, dye-sensitized solar cells, isomers, oligothiophene, quasi-solid state, sensitizers*

INTRODUCTION

Dye-sensitized nanocrystalline TiO_2 solar cells (DSSCs) have been extensively studied since the pioneering work by O'Regan and Grätzel in 1991.[1] The heart of such a device is a photoanode, which is based on a nanocrystalline TiO_2 film covered by a monolayer of photosensitizing dye.[2,3] Upon optical excitation, the chemically adsorbed dye molecules on the surface inject electrons into the conduction band (CB) of the mesoporous TiO_2. Then, the electrons are brought back to the oxidized dye through an external circuit, a platinum counter electrode, and a redox system.[2] Up to date, such cells employing mostly ruthenium polypyridyl complexes as sensitizers have achieved power conversion efficiency (η) over 10% under standard global air mass of 1.5.[4−9] Recently, DSSC devices showing a new η record of 12.3% have been achieved with zinc-porphyrin dye YD2-o-C8 cosensitized with an organic dye Y123 using cobalt-based electrolyte.[10] Meanwhile, metal-free organic dyes, commonly constructed with donor-π bridge-acceptor (D-π-A) configuration, have also attracted considerable attention for practical applications owing to their lower cost of production and better flexibility in terms of molecular tailoring with respect to classical ruthenium polypyridine complexes.[11]

In the past decade, many kinds of organic dyes with such configuration have been explored for DSSCs, including sensitizers based on thiophene,[12−26] furan,[27,28] selenophene,[29] and pyrrole[30] derivatives, and impressive efficiency over 8% has been achieved in liquid electrolyte systems.[16,19,31−40] Although great efforts have been devoted to the modification and optimization of the sensitizer structures, most of the efficient metal-free organic dyes consist of thiophene or its derivative. However, it is well known that the molecules containing thiophene or oligothiophene are quite easy to form intermolecular aggregation due to their planar structures.[20,41] As a result, the excited electrons in the photoanode will recombine with another oxidized dye molecule. Such interfacial charge carrier recombination may cause an open-circuit voltage (V_{oc}) reduction, hence decreasing the photoelectric conversion

Received: May 28, 2013
Accepted: August 27, 2013
Published: August 27, 2013

   dx.doi.org/10.1021/am402036j | ACS Appl. Mater. Interfaces 2013, 5, 8982−8990

efficiency. Therefore, the suppression of dye aggregation is of vital importance for achieving improvements in device performance.

Introduction of alkyl chains to the dye skeleton based on thiophene or its derivative has proved to be an effective method to improve the DSSC performance since they can not only prevent dye aggregation but also diminish the charge recombination between electrons and electron acceptors in the electrolyte.[12,20,22,42−45] The success of MK2[20] related sensitizers with linear hexyl groups is a good example. According to our recent research,[46] when branched alkyl chains are introduced into organic sensitizers instead of linear alkyl groups, the DSSCs demonstrate significantly improved photovoltaic performance due to the reduced intermolecular interactions and retarded charge recombination rate. Therefore, herein, two series of isomeric sensitizers (Chart 1) with linear

Chart 1. Molecular Structures of Dye Isomers

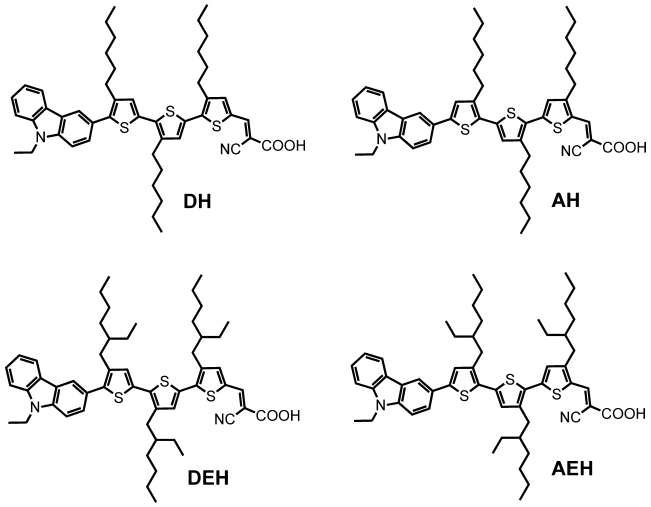

n-hexyl and branched 2-ethylhexyl chains have been designed and synthesized. The sensitizers are referred according to their different chemical structures. In the **D** (donar) series sensitizers, alkyl chains are introduced into the terthiophene spacer closer to the donor moiety, while for the **A** (anchor) series dyes, the incorporated alkyl chains are closer to the anchor group. "**H**" and "**EH**" represent the substituted *n*-hexyl and 2-ethylhexyl on the terthiophene spacer, respectively. The optoelectronic property difference between the isomers is characterized by UV−vis absorption spectroscopy, cyclic voltammetry (CV), and photovoltaic measurements. The results illustrate the subtlety of the structure/function relationship in DSSCs based on those isomers. In the case of **A** series dyes, a remarkable bathochromic shift in absorption maximum and a higher molar extinction coefficient in chloroform solutions were observed in comparison with **D** series dyes; hence, a broader IPCE curve and a higher short-circuit current were obtained. **D** series isomers with more twisted structures exhibit a longer electron lifetime and lower charge recombination rate by a more effective blocking effect, which in combination with titania CB movement is responsible for the mild enhancement in V_{oc}. When the the two effects were combined, a significant enhancement in conversion efficiency was achieved through switching the 2-ethylhexyl chains from the "left" side to the "right" side and an efficiency of up to 7.10% and 8.66% was obtained for isomer **AEH** sensitized solar cell with quasi-solid-state and liquid electrolyte, respectively.

EXPERIMENTAL SECTION

Materials and Reagents. All of the chemicals and reagents were purchased from J&K Chemical Ltd, China and used as received. Tetrahydronfuran (THF) was distilled from sodium benzophenone ketyl. Chloroform and dichloromethane (CH_2Cl_2) were distilled from CaH_2. All reactions and manipulations were carried out under N_2 with the use of standard inert atmosphere and Schlenk techniques. 3,4′,4″-Tris(*n*-hexyl)-[2,2′,5′,2″]terthiophene **1a** and 3,4′,4″-tris(2-ethylhexyl)-[2,2′,5′,2″]terthiophene **1b** were synthesized according to the literature.[47]

Characterization. The UV−vis absorption spectra of the dye solutions and the dye-loaded transparent films were recorded on a UV-2550PC spectrophotometer (Shimadzu). The PL spectra of the dye solutions were recorded on a RF-5301PC spectrofluorophotometer (Shimadzu). Electrochemical redox potentials were obtained by cyclic voltammetry (CV) measurements, which were performed on a CH electrochemical workstation (CHI604D) using a typical three-electrode electrochemical cell in a solution of tetrabutylammonium hexafluorophosphate (0.1 M) in anhydrous acetonitrile at a scan rate of 50 mV s^{-1} at room temperature under nitrogen. Dye-adsorbed TiO_2 film (5 μm thickness, 0.25 cm^2) on conductive glass was used as the working electrode, a Pt wire as the counter electrode, and an Ag/Ag^+ electrode as the reference in anhydrous acetonitrile. The potential of the reference electrode was calibrated with ferrocene, and all potentials mentioned in this work are against the normal hydrogen electrode (NHE).

Synthesis of Sensitizers. The synthetic details and the characterization of the sensitizers are described in the Supporting Information.

Fabrication of Dye-Sensitized Solar Cells. Fluorine-doped SnO_2 glass (15 Ω/sq, Nippon Sheet Glass) substrates were cleaned in a detergent solution by an ultrasonic bath, washed with acetone and water, and then dried using N_2 current. Nanocrystalline TiO_2 films 12 μm, consisting of a 6 μm transparent layer (~20 nm nanoparticles) and a 6 μm scattering layer (~100 nm particles), in thickness, were prepared using a screen printing technique,[48] followed by sintering at 450 °C under an air flow. After cooling, the TiO_2 films were impregnated in a 0.05 M aqueous $TiCl_4$ solution for 30 min at 70 °C and then rinsed with deionized water. The $TiCl_4$-treated TiO_2 films were annealed at 450 °C for 30 min and then cooled to 100 °C before being immersed into the dye solution for 16 h to allow the dye to adsorb to the TiO_2 surface. After the adsorption of the dyes, the electrodes were rinsed with chloroform and acetonitrile. The resulting photoelectrode and Pt-counter electrodes were assembled into a sealed sandwich solar cell with a thermoplastic frame (Surly 30 μm thick). The cobalt (II/III)-based redox electrolyte consisted of a solution of 0.22 M $[Co^{2+}(bpy)_3](PF_6)_2$, 0.05 M $[Co^{3+}(bpy)_3](PF_6)_3$, 0.1 M $LiClO_4$, and 0.3 M *tert*-butylpyridine (TBP) in acetonitrile.[49] The quasi-solid-state gel electrolyte was prepared by mixing 5 wt % poly(vinylidenefluoride-*co*-hexafluoropropylene) with a redox solution containing a 0.1 M LiI, 0.05 M I_2, 0.5 M TBP, and 0.6 M 1,2-dimethyl-3-propylimidazolium iodide (DMPImI) in 3-methoxypropionitrile (MPN) under heating at 100 °C until all solids were dissolved. After introducing the cobalt(II)/(III)-based liquid electrolyte or the hot gel solution into the internal space of the cell from the two holes predrilled on the back of the counter electrode, the holes were sealed with a Surlyn film covered with a thin glass slide under heat.

Photovoltaic Measurements. The current density−voltage (*J*−*V*) characteristics of the DSSCs were measured by recording *J*−*V* curves using a Keithley 2400 source meter under the illumination of AM1.5G simulated solar light coming from a solar simulator (Oriel-91193 equipped with a 1000 W Xe lamp and an AM1.5 filter). The DSSCs were fully covered with a black mask with an aperture area of 0.2304 cm^2 during measurements. The incident light intensity was calibrated with a standard silicon solar cell (Newport 91150). The electron lifetimes were measured with intensity modulated photovoltage spectroscopy (IMVS),[50−53] whereas charge densities at open-

Scheme 1. Synthetic Routes for D and A Series Dye Isomers[a]

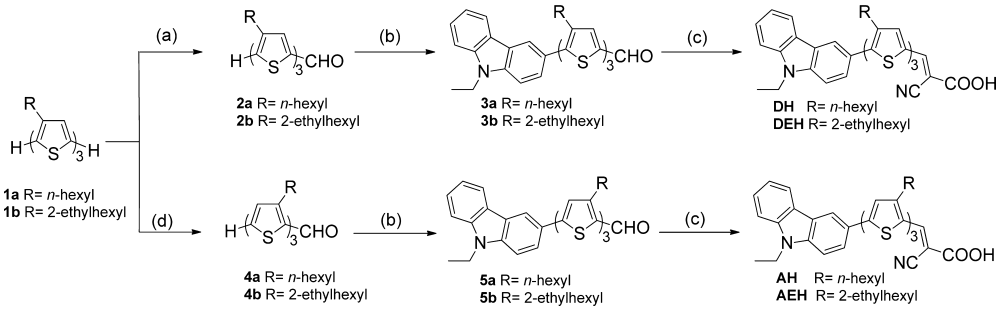

[a]Reagents and conditions: (a) i. *n*-BuLi, THF, −78 °C, 2 h; ii. DMF, to rt, 8 h; iii. 1 M HCl; (b) K_2CO_3, $Pd(OAc)_2$, $PCy_3{\cdot}HBF_4$, pivalic acid, toluene, 110 °C, 16 h; (c) cyanoacetic acid, piperidine, acetonitrile, reflux, 6 h; (d) $POCl_3$, DMF, chloroform, reflux, 20 h.

circuit were measured using charge extraction technique.[54] IMVS analysis and charge extraction were carried out on an electrochemical workstation (Zahner XPOT, Germany), which includes a white light emitting diode and corresponding control system. The intensity-modulated spectra were measured at room temperature with light intensity ranging from 20 to 120 W m^{-2}, in modulation frequency ranging from 0.1 Hz to 10 kHz, and with modulation amplitude less than 5% of the light intensity. Three identical devices were tested in each case with standard deviation less than 5%. Action spectra of the incident monochromatic photon-to-electron conversion efficiency (IPCE) for the solar cells were obtained with an Oriel-74125 system (Oriel Instruments). The intensity of monochromatic light was measured with a Si detector (Oriel-71640).

RESULTS AND DISCUSSION

Synthesis and Characterization. The straightforward synthetic routes to the dye isomers are depicted in Scheme 1. The synthetic procedure for both **D** and **A** dye isomers started from "head-to-tail" alkylated terthiophene.[47] For the **D** series isomers, lithiation of starting materials **1a** and **1b** with a stoichiometric amount of *n*-butyllithium at −78 °C followed by quenching with *N*,*N*-dimethylformamide and subsequent acidic hydrolysis produced the corresponding monoaldehyde-substituted derivatives **2a** and **2b**, respectively. The successful incorporation of aldehyde group on the "right" side was validated by the disappearance of two doublet peaks in the ^{1}H NMR spectrum for the starting material and the appearance of a new singlet peak at δ = 7.58 or 7.54 ppm in the ^{1}H NMR spectrum for the product. Electron donor, *N*-ethylcarbazole, was attached via a recently developed C−H bond activation,[55] which shortened the synthetic procedure by two steps. Otherwise, oligothiophene bromide and boronic acid reagents have to be prepared before a Pd-catalyzed cross coupling reaction. In the last step, the obtained precursors were converted to dyes **DH** and **DEH** by Knoevenagel condensation[56] with cyanoacetic acid in refluxing acetonitrile in the presence of piperidine. While for the **A** series isomers, the aldehyde group was introduced by refluxing starting compound **1** with a Vilsmeier reagent. Thus, the alkyl groups were located on the "right" side of the oligothiophene spacer. The introduction of aldehyde group on the other side was proved by the disappearance of one singlet peak at δ = 6.89 or 6.86 ppm in the ^{1}H NMR spectrum for the starting material. Similar to the **D** series dye isomers, electron donor, i.e., *N*-ethylcarbazole, and anchor group, i.e., cyanoacetic acid, were attached via C−H bond activation and Knoevenagel condensation, respectively, which eventually produced the **A** series dye isomers. The target isomeric compounds were characterized by ^{1}H NMR spectroscopy, ^{13}C NMR spectroscopy, and mass spectroscopy and were found to be consistent with the proposed structures. It should be noted that, compared with the developed synthetic route for sensitizer MK1, which was stepwise constructed by around 10 steps,[20,57] our synthetic procedure for each sensitizer contains only three steps starting from the oligothiophene spacer. Therefore, when several series of organic sensitizers have to be synthesized for comparison of photovoltaic properties or a highly efficient organic sensitizer has to be produced in a large scale, our straightforward synthetic steps will dramatically shorten the synthesis steps and facilitate the synthetic work.

Optical Properties. The obtained dye isomers are brown in the solid state and can freely dissolve in chloroform, THF, and toluene to produce orange or red solutions. The electronic absorption spectra of the four isomers in chloroform solutions are shown in Figure 1, and the characteristic data are collected

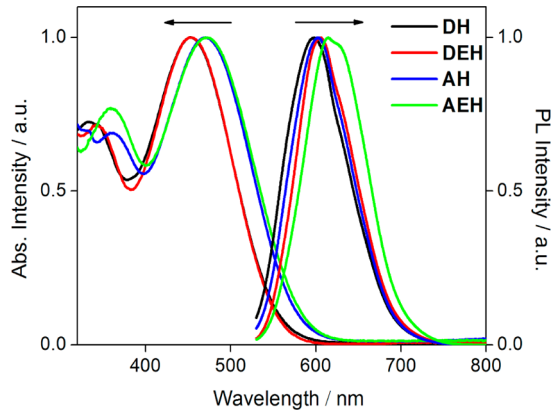

Figure 1. Normalized UV−vis absorption and PL spectra of the dye isomers in chloroform solutions.

in Table 1. All of the dyes exhibit their major electronic absorption bands in the visible region (400−600 nm) due to the intramolecular charge transfer (ICT) from the donor to the acceptor. Additionally, another much weaker absorption band can be observed for all dyes in the ultraviolet region (300−400 nm), which is assigned to the π−π^* electron transition of the conjugated backbone. As shown in Figure 1, the chloroform solution (ca. 5 × 10^{-6} M) of dye **DH** displays the maximum absorption band at 453 nm (ε = 2.86 × 10^4 M^{-1} cm^{-1}). Upon replacing the subsituted *n*-hexyl with 2-ethylhexyl groups on the terthiophene spacer, dye **DEH** exhibits a similar absorption spectrum with the maximum absorption wavelength at 451 nm

dx.doi.org/10.1021/am402036j | ACS Appl. Mater. Interfaces 2013, 5, 8982−8990

Table 1. Photophysical and Electrochemical Properties of the Dye Isomers

dye	λ_{max}^{Abs}, nm[a]	ε, M^{-1} cm^{-1}	λ_{max}^{Abs} on TiO_2, nm	Γ[b], mol cm^{-2} μm^{-1}	λ_{max}^{PL}, nm	Stokes shift, cm^{-1}	HOMO, V[c]	$E_{0\text{-}0}$, eV	LUMO, V
DH	453	2.86×10^4	439	1.4×10^{-8}	598	5353	1.08	2.15	−1.07
DEH	451	2.51×10^4	438	1.2×10^{-8}	606	5671	1.09	2.14	−1.05
AH	471	3.19×10^4	454	1.9×10^{-8}	603	4648	1.00	2.08	−1.08
AEH	470	2.85×10^4	454	1.5×10^{-8}	615	5016	1.03	2.03	−1.00

[a]Absorption peaks (λ_{max}) and molar extinction coefficients (ε) were measured in chloroform solutions (~5×10^{-6} M). [b]Γ is the surface concentration of the dye on the TiO_2 film. [c]The potentials (vs. NHE) were calibrated with ferrocene.

($\varepsilon = 2.51 \times 10^4$ M^{-1} cm^{-1}) in chloroform solution. The similar absorption maxima are not difficult to be understood as **DH** and **DEH** have almost identical chemical structures except for the additional ethyl groups attached on the hexyl substituents. This phenomenon is close to our recently published results.[44,58] Under the same condition, the chloroform solutions of **AH** and **AEH** demonstrate the absorption maximum at 471 nm ($\varepsilon = 3.19 \times 10^4$ M^{-1} cm^{-1}) and 470 nm ($\varepsilon = 2.85 \times 10^4$ M^{-1} cm^{-1}), respectively. However, when the alkyl groups shift from the "left" side of isomer **DH** to the "right" side of isomer **AH**, a significant bathochromic shift of 18 nm along with increased absorption intensity of the maximum absorption band can be clearly observed. Similarly, for isomers **DEH** and **AEH**, a bathochromic shift (19 nm) and increased absorption intensity are also observed. Such bathochromically shifted maximum absorption wavelength and the increased molar extinction coefficient value are attributed to the extended effective conjugation length. In the **D** series sensitizers, a steric hindrance exists between the alkyl chains and the carbazole unit, resulting in a backbone twist between the carbazole donor and the oligothiophene spacer, which therefore weakens the π-conjugated system in comparison to the **A** series dyes. Moreover, it should be noted that the twisted molecular structures in **D** series sensitizers have suppressed the intermolecular interactions more effectively in comparison to **A** series sensitizers. To study the intermolecular interactions of the resulted dye isomers, the absorption spectra for the sensitizers with different concentrations were recorded and displayed in Figure S1, Supporting Information. With the concentration increasing from 5×10^{-6} to 5×10^{-4} M, no obvious shift for the maximum wavelength can be observed for sensitizer **DEH**, while the maximum absorption wavelength for sensitizer **AEH** bathochromically shifts from 470 to 497 nm due to the intermolecular aggregation. This indicates that stronger intermolecular interactions exist in the **A** series isomeric dyes in comparison to the **D** series dye isomers.

The photoluminescence (PL) spectra of the isomeric dyes in chloroform solutions were recorded, and the corresponding data are summarized in Table 1. As shown in Figure 1, the maximum PL wavelength is located at 598 nm for **DH**, while it bathochromically shifts to 606 nm for **DEH**. While for the **A** series dyes, the maximum PL wavelength bathochromically shifts from 603 nm for **AH** to 615 nm for **AEH**. Large Stokes shift (4648−5671 cm^{-1}) can be observed for all the sensitizer isomers, which is attributed to the charge transfer nature of the excited state.[59] However, a more planar conformation of the excited state may also contribute to the smaller Stokes shift.[59] Herein, **DH** and **DEH** exhibit more twisted structure conformation caused by the introduction of alkyl groups closed to the bulky carbazole moiety. Therefore, **DH** and **DEH** display larger Stokes shifts in comparison to those for **AH** and **AEH**, respectively.

Figure 2 shows the absorption spectra of the organic sensitizers anchored to a transparent mesoporous TiO_2 film.

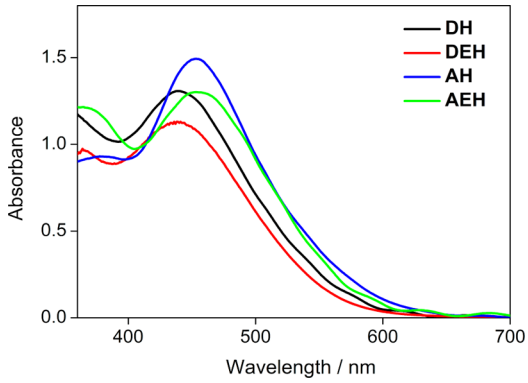

Figure 2. UV−vis absorption spectra of the dye isomers on transparent titania films.

Adsorption of the organic dyes on the surface of the TiO_2 films broadens their absorption spectra, and a hypsochromic shift of 13−17 nm with respect to those in solutions was observed, which could be owing to the deprotonation of the carboxylic acid. Such hypsochromic shift of the absorption spectra for organic dyes adsorbed on the TiO_2 films has also been observed in other metal-free organic dyes.[15,60−63] Similarly, when the positions of the alkyl chains are varied from the "left" side to "right" side, an obvious bathochromical shift for the maximum absorption band can be found. This is consistent with the absorption spectra in solutions and originates from the different effective conjugation length. Moreover, the absorption intensity of **A** series dye loaded TiO_2 film is higher than corresponding **D** series dye loaded TiO_2 film. This can be explained by the dye loading amount which was measured by UV−vis absorption spectroscopy through desorption of sensitizer from the dye-loaded TiO_2 film. As shown in Table 1, **A** series dyes possessed a higher dye loading amount than the corresponding **D** series counterpart. Furthermore, the organic sensitizers containing 2-ethylhexyl groups showed a lower dye loading amount than the ones with *n*-hexyl groups due to the excessive bulkiness of branched 2-ethylhexyl substituents. This explains the relatively higher absorbance of *n*-hexyl substituted organic dye loaded film in comparison to that loaded with 2-ethylhexyl subsituted sensitizers.

Electrochemical Properties. To determine the oxidation potential of the organic dyes and thermodynamically evaluate the possibility of sensitizer regeneration, CV was carried out in a typical three-electrode electrochemical cell with TiO_2 films stained with sensitizer as the working electrode, Pt wire as the counter electrode, and Ag/Ag^+ as the reference electrode dipped in a solution of tetrabutylammonium hexafluorophosphate (0.1 M) in water-free acetonitrile at a scan rate of 50 mV s^{-1} at room temperature. As shown in Figure 3, both **D** and **A**

dx.doi.org/10.1021/am402036j | ACS Appl. Mater. Interfaces 2013, 5, 8982−8990

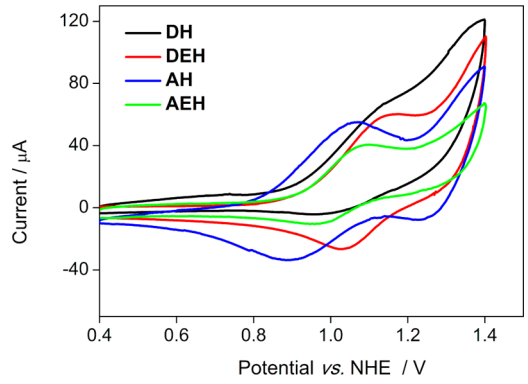

Figure 3. Cyclic voltammograms of the isomeric dye loaded TiO_2 films (5 μm thickness, 0.25 cm^2).

dyes exhibit one oxidative wave attributed to the oxidation of the carbazole moiety. The energy levels of the isomeric dye-sensitized electrodes are summarized in Table 1. The observed oxidation potential is taken as the highest occupied molecular orbital (HOMO) level. All the HOMO values are more positive than I^-/I_3^- redox couples (~0.40 V vs. NHE, same below),[3] indicating that the reduction of the oxidized dyes with I^- ions is thermodynamically feasible. Interestingly, the oxidation potentials of **A** dyes slightly shift cathodically in comparison with that of **D** dyes. In the **D** series dyes, the molecular twist causes worse conjugation and charge delocalization. Therefore, **D** series isomers possess less π conjugation and, in turn, more positive oxidation potential. The lowest unoccupied molecular orbital (LUMO) energy level was estimated from the equation LUMO = HOMO − ΔE, where ΔE is the gap between the HOMO and LUMO levels and is derived from the wavelength at 10% maximum absorption intensity for the dye-loaded TiO_2 film.[64] Correspondingly, the LUMO energy levels of all sensitizers are more negative than the CB edge of TiO_2 electrode (−0.5 V),[3] thus providing a sufficient thermodynamic driving force for the electron injection from their excited states to TiO_2 films.

Theoretical Approach. To gain insight into the geometrical and electronic properties of the isomeric sensitizers, density functional calculations were conducted using the Gaussian 03 program package at the B3LYP/6-31G(d) level (Figure S2, Supporting Information).[65] It can be clearly found that, for all sensitizers, the HOMO was distributed along the conjugated system and the LUMO was delocalized over the cyanoacrylic acid group through alkylated oligothiophene, facilitating electron transfer from the excited state to the CB of TiO_2 via the carboxylate anchoring group. Furthermore, the presence of strong electron density relocation between HOMO and LUMO supports the occurrence of an intramolecular charge transfer transition in the UV−vis spectra.[66]

It is worth noting that the dihedral angle between the carbazole donor and the neighbored thiophene ring is distinct for the **D** and **A** series isomers. As shown in Figure 4, the dihedral angles between the carbazole and the neighbored thiophene ring in **AH** and **AEH** are calculated to be 26° and 27°, respectively, which is a generalized observation for dihedral angle between benzene and thiophene rings. However, the **D** series dyes show a more twisted dihedral angle of 47° and 51° for **DH** and **DEH**, respectively, due to the large steric effect between the alkyl chain and carbazole unit. On the other hand, no significant difference can be observed for the dihedral angles

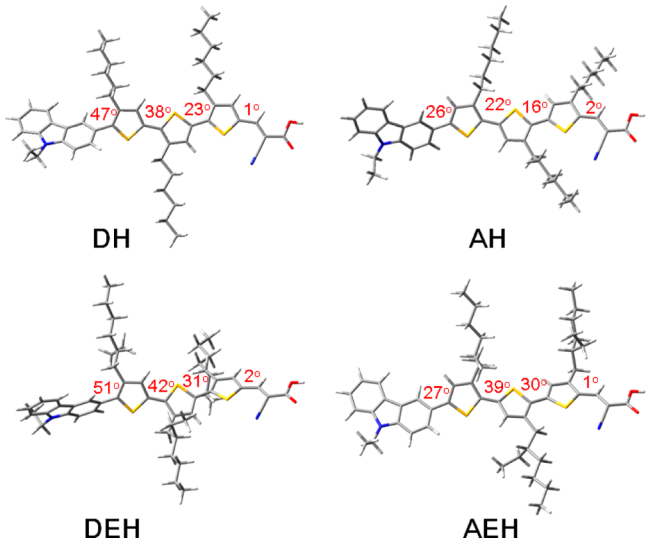

Figure 4. Optimized ground-state geometries and dihedral angles between the π-planes of **D** and **A** series dye isomers.

between the vinylene and the neighbored thiophene ring. Consequently, **D** series isomers possess more twisted conjugation backbone, which may perturb the effective π-conjugation of the dye molecules, accounting for the hypsochromic shift of the maximum absorption band in the absorption spectra of the **D** series dyes in comparison to those for the **A** series sensitizers.

Solar Cell Performance. Quasi-solid-state DSSCs have shown greatly improved long-term stability since there is less or no possibility for leakage of the electrolyte.[67,68] Therefore, the isomeric sensitizer-based quasi-solid-state DSSCs are firstly constructed using a quasi-solid-state gel electrolyte containing 5 wt % poly(vinylidenefluoride-*co*-hexafluoropropylene),[69] 0.1 M LiI, 0.05 M I_2, 0.5 M TBP, and 0.6 M DMPImI in MPN. Figure 5a displays the *J*−*V* curves of the DSSCs using such quasi-solid-state gel electrolyte under simulated AM1.5G irradiation. The DSSC based on **DH** produces a η of 5.03% (J_{sc} = 9.19 mA cm^{-2}, V_{oc} = 771 mV, FF = 0.71), while **DEH**-based DSSC provides a slightly decreased η of 4.63% (J_{sc} = 8.49 mA cm^{-2}, V_{oc} = 791 mV, FF = 0.69), which is consistent with our recently published results.[56] Upon replacing the alkyl groups from the "left" side to the "right" side, the device incorporating **A** series dye gives a η of 6.18% for **AH** (J_{sc} = 11.54 mA cm^{-2}, V_{oc} = 754 mV, FF = 0.71) and a η of 7.10% for **AEH** (J_{sc} = 12.81 mA cm^{-2}, V_{oc} = 770 mV, FF = 0.72), respectively. For the **A** series dye-based DSSCs, the J_{sc} values significantly increase while the V_{oc} values slightly decrease as compared with those for the DSSCs based on the **D** series dye. Therefore, the contribution to the η values from the J_{sc} parameter is much more significant than the V_{oc} parameter. Consequently, the DSSCs based on **A** series dyes showed more prominent power conversion efficiency than those for **D** series dye-based DSSCs. However, unlike the **D** series dye-based DSSC, **AEH**-based DSSC produces a much higher efficiency as compared with **AH**-based DSSC. This is probably due to the less twisted structures for **A** series dyes in comparison to **D** series dyes, which results in much stronger intermolecular interactions in **A** series dyes. Therefore, for organic dye with a relatively planar structure, 2-ethylhexyl groups are superior to *n*-hexyl groups in inhibiting the intermolecular interactions and thus improving the DSSC performance.

dx.doi.org/10.1021/am402036j | ACS Appl. Mater. Interfaces 2013, 5, 8982−8990

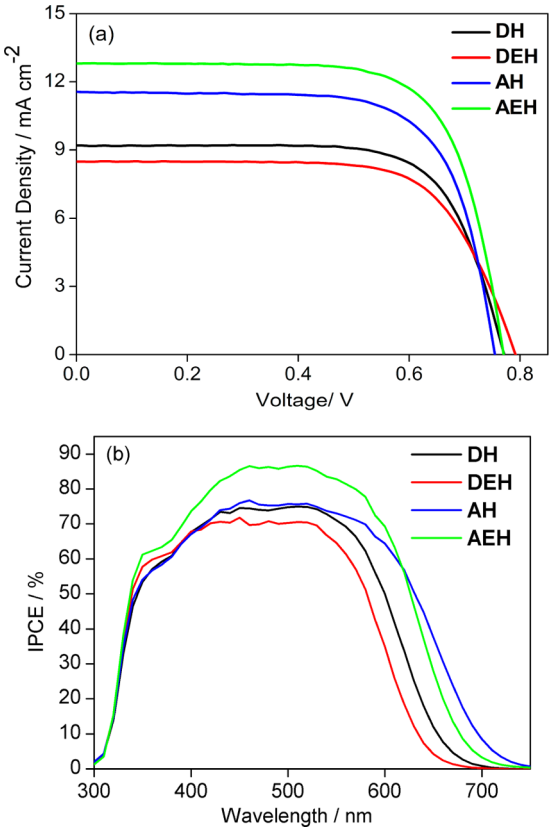

Figure 5. (a) J–V curves and (b) IPCE spectra for the quasi-solid-state DSSCs based on the isomeric sensitizers.

To understand the significant difference among the J_{sc} values and further investigate the relationship between the sensitizer structure and the photovoltaic performance, action spectra of the incident photon-to-current conversion efficiencies (IPCE) as a function of incident wavelength for the quasi-solid-state DSSCs based on the isomeric sensitizers are recorded and shown in Figure 5b. It can be found that the IPCE spectra for all quasi-solid-state DSSCs are in good agreement with their absorption spectra, displaying the highest value of around 85%. Typically, the IPCE spectra for the DSSCs based on the **A** series sensitizers are much broader than those for the **D** series isomer-based DSSCs. This is obviously due to the more planar chemical structures of the **A** series dyes, which therefore induces a more effective π-conjugation and is beneficial to the light-harvesting capability.

Since V_{oc} is related to the CB position of TiO_2 and the charge recombination rate in DSSCs, in order to explain the difference of another important performance parameter (V_{oc}), the CB positions of the isomeric dye loaded TiO_2 films were investigated through charge extraction and intensity modulated photovoltage spectroscopy (IMVS) measurements.[50−53] According to the method developed by Frank and co-workers,[50,70,71] the movement of CB is contributed to the change in V_{oc} at constant photoinduced charge density (Q), which was measured with charge extraction technique[54] under illumination of a white light from LED. A higher V_{oc} at constant Q indicates an upward (or negative) shift of the CB edge and vice versa.[71] A plot of V_{oc} versus the charge density at open circuit for the quasi-solid-state DSSCs is shown in Figure 6. It can be found that the V_{oc} increases linearly with the logarithm of Q for all DSSCs and the four curves for the corresponding devices

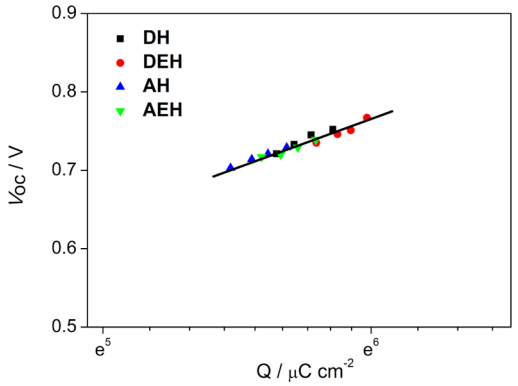

Figure 6. V_{oc} as a function of charge density at open circuit for quasi-solid-state DSSCs based on the isomeric sensitizers.

have almost the same slope (114 mV). At a fixed Q, the almost same V_{oc} for all DSSCs indicates the identical CB position for each case. Consequently, CB edge of the TiO_2 semiconductor remains unchanged upon the adsorption the dye isomers with alkyl chains on the "left" side or the "right" side. As the changes in the chemical structures of the dye isomers do not induce the movement of the TiO_2 CB, the V_{oc} difference among the resulted quasi-solid-state DSSCs should be attributed to the repression of charge recombination, which is related to electron lifetime (τ). Figure S3, Supporting Information, shows the electron lifetime as a function of charge density at open circuit for the DSSCs based on the four sensitizers. The electron lifetime was obtained from the frequency at the top of the semicircle (f_{min}) in IMVS by the relation $\tau = (2\pi f_{min})^{-1}$. As illustrated in Figure S3, Supporting Information, the quasi-solid-state DSSCs based on **DH** and **DEH** show 4.5 and 3.4 times longer electron lifetime at a certain charge density in comparison to those based on **AH** and **AEH**, respectively, which is attributed to the attenuated charge recombination. This indicates that **D** series isomers with more twisted structures can suppresses the charge recombination between electrons in TiO_2 film and electron acceptors in the electrolyte more efficiently than **A** series counterparts.

Finally, to investigate the effect of twisted structure formed between the carbazole donor and π-spacer on charge recombination rate, charge recombination current (J_r) at open circuit is plotted against charge density (Figure S4, Supporting Information). At open circuit and a fixed light intensity, the recombination current density J_r equals the charge-injection current density J_{inj}. However, neither of them can be directly measured but can be estimated from the measurement of J_{sc}. At short-circuit, J_r is taken as J_{sc} in value under the same light intensity because of the negligible charge recombination at short-circuit.[72−74] At a given charge density, the charge recombination current is 2.8 times larger for the quasi-solid-state DSSC based on **AH** than that for **DH**-based DSSC, while it is 2.9 times larger for the **AEH**-based quasi-solid-state DSSC than that for the **DEH**-based device, indicating that the recombination rate constant is thus reduced significantly when the positions of the alkyl chains are varied from the "right" side to "left" side. The retarded charge recombination rate constant will reduce electron loss at open circuit. When more charge is accumulated in TiO_2, Fermi level moves upward and V_{oc} gets larger. According to the Q–V_{oc} plots, the V_{oc} gain from the **AEH**-based DSSC to the **DH**, **DEH**, and **AH**-based DSSCs arising solely from the increased

dx.doi.org/10.1021/am402036j | ACS Appl. Mater. Interfaces 2013, 5, 8982−8990

charge density or retarded charge recombination is calculated to be 6, 17, and −12 mV, respectively, explaining why the V_{oc} difference between **AEH**-based DSSS and those based on **DH**, **DEH**, and **AH** is 1, 21, and −16 mV, respectively.

The quasi-solid-state devices were tested to evaluate the long-term stability under visible light soaking. Figure 7 displays

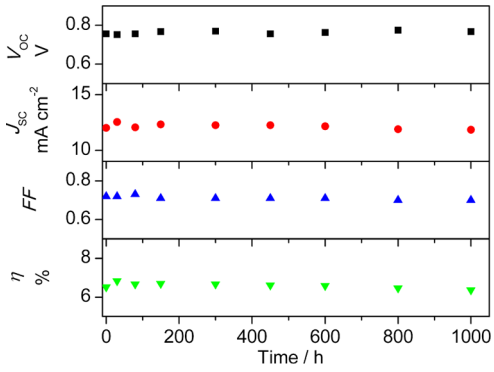

Figure 7. Evolutions of photovoltaic performance parameters for **AEH**-based quasi-solid-state DSSC during one sun soaking.

the variation in the photovoltaic parameters of quasi-solid-state DSSC based on isomer **AEH** under one sun soaking. It can be found that the overall efficiency remained 98% of its initial value after 1000 h of visible-light soaking, which indicates that the quasi-solid-state DSSCs based on **AEH** demonstrated good long-term stability during light soaking. Therefore, sensitizer **AEH** is a promising candidate for highly efficient and stable quasi-solid-state DSSC.

Recently, the DSSCs using a Co(II)/(III)-based redox couple have become a research hotspot in this area due to its more positive redox potential which is favorable for high V_{oc} and hence η values.[10,75] Therefore, the DSSCs based on the resulted isomeric sensitizers were also fabricated with a liquid electrolyte (0.22 M $[Co^{2+}(bpy)_3](PF_6)_2$, 0.05 M $[Co^{3+}(bpy)_3](PF_6)_3$, 0.1 M $LiClO_4$, and 0.3 M TBP in acetonitrile).[49] The corresponding current density−voltage (J−V) curves of the DSSCs were recorded under simulated AM1.5G irradiation (100 mW cm^{-2}) and shown in Figure S5, Supporting Information. The DSSCs based on **DH** and **DEH** produced a J_{sc} of 11.40 and 9.37 mA cm^{-2}, a V_{oc} of 835 and 857 mV, and an FF of 0.67 and 0.75, corresponding to a η of 6.38% and 6.02%, respectively. Under the same condition, replacing the corresponding alkyl chains from the "left" side to the "right" side, the DSSCs fabricated with **AH** and **AEH** produced increased J_{sc} values but decreased V_{oc} values (Table 2) in comparison to those for **D** series dye-based DSSCs. Notably, a J_{sc} of 14.98 mA cm^{-2}, a V_{oc} of 814 mV, and an FF of 0.71, corresponding to a η of 8.66%, was achieved for **AEH**-based DSSC. Obviously, the photovoltaic performance of the DSSCs using Co(II)/(III)-based liquid electrolyte is consistent with the trend for the DSSCs based on quasi-solid-state electrolyte discussed above.

Table 2. Photovoltaic Performance of the DSSCs Based on Liquid Electrolyte Containing Co(II)/(III) Redox Couple

dye	J_{sc}, mA cm^{-2}	V_{oc}, mV	FF	η, %
DH	11.40	835	0.67	6.38
DEH	9.37	857	0.75	6.02
AH	12.30	799	0.73	7.17
AEH	14.98	814	0.71	8.66

CONCLUSIONS

In summary, we have developed a facile and selective synthesis approach towards organic dye isomers with alkyl groups substituted at different positions on the terthiophene bridge. The effects of isomeric structures on photophysical and electrochemical properties and DSSC performance have been fully investigated. The **D** series isomeric dyes with more twisted molecular skeleton have suppressed the intermolecular interactions more effectively and retarded the charge recombination more efficiently. Therefore, the DSSCs based on the **D** series dyes exhibit a longer electron lifetime with lower charge recombination rate, which results in the enhanced V_{oc} values, while the **A** series isomers demonstrate more planar geometry configuration and more effective π-conjugation, inducing bathochromically shifted absorption maxima and improved light-harvesting ability in comparison to the **D** series isomers. Consequently, the DSSCs based on the **A** series dyes illustrate broadened IPCE spectra and enhanced J_{sc} values. Overall, the contribution to the η values from the photocurrent is more remarkable than that from the photovoltage. As a result, a η of 7.10% and 8.66%, respectively, is achieved for isomer **AEH**-based DSSC using quasi-solid-state and liquid electrolyte, respectively. The η of the former quasi-solid-state DSSC remained 98% of the initial value after continuous light soaking for 1000 h.

ASSOCIATED CONTENT

Supporting Information

Synthesis and characterization details for the dye isomers and characterization of the DSSCs based on the isomeric sensitizers. This material is available free of charge via the Internet at http://pubs.acs.org.

AUTHOR INFORMATION

Corresponding Authors

*E-mail: zhougang@fudan.edu.cn. Tel: +86-21-5163-0345. Fax: +86-21-5163-0345.

*E-mail: zs.wang@fudan.edu.cn. Tel: +86-21-5163-0345. Fax: +86-21-5163-0345.

Notes

The authors declare no competing financial interest.

ACKNOWLEDGMENTS

This work was financially supported by the National Basic Research Program (2011CB933302) of China, the National Natural Science Foundation of China (90922004 and 51273045), NCET-12-0122, Shanghai Pujiang Project (11PJ1401700), STCSM (12JC1401500), Shanghai Leading Academic Discipline Project (B108), and Jiangsu Major Program (BY2010147).

REFERENCES

(1) O'Regan, B.; Grätzel, M. *Nature* **1991**, *353*, 737−740.

(2) He, J.; Benkö, G.; Korodi, F.; Polívka, T.; Lomoth, R.; Åkermark, B.; Sun, L.; Hagfeldt, A.; Sundström, V. *J. Am. Chem. Soc.* **2002**, *124*, 4922−4932.

(3) Hagfeldt, A.; Grätzel, M. *Chem. Rev.* **1995**, *95*, 49−68.

(4) Nazeeruddin, M. K.; De Angelis, F.; Fantacci, S.; Selloni, A.; Viscardi, G.; Liska, P.; Ito, S.; Takeru, B.; Grätzel, M. G. *J. Am. Chem. Soc.* **2005**, *127*, 16835−16847.

(5) Grätzel, M. *J. Photochem. Photobiol., C: Photochem. Rev.* **2003**, *4*, 145−153.
(6) Gao, F.; Wang, Y.; Shi, D.; Zhang, J.; Wang, M. K.; Jing, X. Y.; Humphry-Baker, R.; Wang, P.; Zakeeruddin, S. M.; Grätzel, M. *J. Am. Chem. Soc.* **2008**, *130*, 10720−10728.
(7) Chen, C. Y.; Wang, M. K.; Li, J. Y.; Pootrakulchote, N.; Alibabaei, L.; Ngoc-le, C. H.; Decoppet, J. D.; Tsai, J. H.; Grätzel, C.; Wu, C. G.; Zakeeruddin, S. M.; Grätzel, M. *ACS Nano* **2009**, *3*, 3103−3109.
(8) Wu, K.-L.; Ku, W.-P.; Clifford, J. N.; Palomares, E.; Ho, S.-T.; Chi, Y.; Liu, S.-H.; Chou, P.-T.; Nazeeruddin, M. K.; Gratzel, M. *Energy Environ. Sci.* **2013**, *6*, 859−870.
(9) Wang, S.-W.; Wu, K.-L.; Ghadiri, E.; Lobello, M. G.; Ho, S.-T.; Chi, Y.; Moser, J.-E.; De Angelis, F.; Gratzel, M.; Nazeeruddin, M. K. *Chem. Sci.* **2013**, *4*, 2423−2433.
(10) Yella, A.; Lee, H. W.; Tsao, H. N.; Yi, C.; Chandiran, A. K.; Nazeeruddin, M. K.; Diau, E. W. G.; Yeh, C. Y.; Zakeeruddin, S. M.; Grätzel, M. *Science* **2011**, *334*, 629−634.
(11) Mishra, A.; Fischer, M. K. R.; Bäuerle, P. *Angew. Chem., Int. Ed.* **2009**, *48*, 2474−2499.
(12) Mao, J.; He, N.; Ning, Z.; Zhang, Q.; Guo, F.; Chen, L.; Wu, W.; Hua, J.; Tian, H. *Angew. Chem., Int. Ed.* **2012**, *51*, 9873−9876.
(13) Wu, Y.; Marszalek, M.; Zakeeruddin, S. M.; Zhang, Q.; Tian, H.; Grätzel, M.; Zhu, W. *Energy Environ. Sci.* **2012**, *5*, 8261−8272.
(14) Cai, S.; Hu, X.; Zhang, Z.; Su, J.; Li, X.; Islam, A.; Han, L.; Tian, H. *J. Mater. Chem. A* **2013**, *1*, 4763−4772.
(15) Choi, H.; Baik, C.; Kang, S. O.; Ko, J.; Kang, M. S.; Nazeeruddin, M. K.; Grätzel, M. *Angew. Chem., Int. Ed.* **2008**, *47*, 327−330.
(16) Yum, J. H.; Hagberg, D. P.; Moon, S. J.; Karlsson, K. M.; Marinado, T.; Sun, L. C.; Hagfeldt, A.; Nazeeruddin, M. K.; Grätzel, M. *Angew. Chem., Int. Ed.* **2009**, *48*, 1576−1580.
(17) Liu, W. H.; Wu, I. C.; Lai, C. H.; Lai, C. H.; Chou, P. T.; Li, Y. T.; Chen, C. L.; Hsu, Y. Y.; Chi, Y. *Chem. Commun.* **2008**, 5152−5154.
(18) Thomas, K. R. J.; Hsu, Y.-C.; Lin, J. T.; Lee, K.-M.; Ho, K.-C.; Lai, C.-H.; Cheng, Y.-M.; Chou, P.-T. *Chem. Mater.* **2008**, *20*, 1830−330.
(19) Wang, Z.-S.; Koumura, N.; Cui, Y.; Takahashi, M.; Sekiguchi, H.; Mori, A.; Kubo, T.; Furube, A.; Hara, K. *Chem. Mater.* **2008**, *20*, 3993−4003.
(20) Nishida, J.-i.; Masuko, T.; Cui, Y.; Hara, K.; Shibuya, H.; Ihara, M.; Hosoyama, T.; Goto, R.; Mori, S.; Yamashita, Y. *J. Phys. Chem. C* **2010**, *114*, 17920−17925.
(21) Xu, M. F.; Li, R. Z.; Pootrakulchote, N.; Shi, D.; Guo, J.; Yi, Z. H.; Zakeeruddin, S. M.; Grätzel, M.; Wang, P. *J. Phys. Chem. C* **2008**, *112*, 19770−19776.
(22) Kim, S.; Lee, J. K.; Kang, S. O.; Ko, J.; Yum, J. H.; Fantacci, S.; De Angelis, F.; Di Censo, D.; Nazeeruddin, M. K.; Grätzel, M. *J. Am. Chem. Soc.* **2006**, *128*, 16701−16707.
(23) Koumura, N.; Wang, Z.-S.; Mori, S.; Miyashita, M.; Suzuki, E.; Hara, K. *J. Am. Chem. Soc.* **2006**, *128*, 14256−14257.
(24) Qin, H.; Wenger, S.; Xu, M.; Gao, F.; Jing, X.; Wang, P.; Zakeeruddin, S. M.; Grätzel, M. *J. Am. Chem. Soc.* **2008**, *130*, 9202−9203.
(25) Liang, Y.; Peng, B.; Liang, J.; Tao, Z.; Chen, J. *Org. Lett.* **2010**, *12*, 1204−1207.
(26) Yang, H.-Y.; Yen, Y.-S.; Hsu, Y.-C.; Chou, H.-H.; Lin, J. T. *Org. Lett.* **2009**, *12*, 16−19.
(27) Kim, S. H.; Kim, H. W.; Sakong, C.; Namgoong, J.; Park, S. W.; Ko, M. J.; Lee, C. H.; Lee, W. I.; Kim, J. P. *Org. Lett.* **2011**, *13*, 5784−5787.
(28) Lin, J. T.; Chen, P.-C.; Yen, Y.-S.; Hsu, Y.-C.; Chou, H.-H.; Yeh, M.-C. P. *Org. Lett.* **2008**, *11*, 97−100.
(29) Li, R. Z.; Lv, X. J.; Shi, D.; Zhou, D. F.; Cheng, Y. M.; Zhang, G. L.; Wang, P. *J. Phys. Chem. C* **2009**, *113*, 7469−7479.
(30) Yen, Y.-S.; Hsu, Y.-C.; Lin, J. T.; Chang, C.-W.; Hsu, C.-P.; Yin, D.-J. *J. Phys. Chem. C* **2008**, *112*, 12557−12567.
(31) Horiuchi, T.; Miura, H.; Sumioka, K.; Uchida, S. *J. Am. Chem. Soc.* **2004**, *126*, 12218−12219.
(32) Ito, S.; Miura, H.; Uchida, S.; Takata, M.; Sumioka, K.; Liska, P.; Comte, P.; Péchy, P.; Grätzel, M. *Chem. Commun.* **2008**, 5194−5196.
(33) Ito, S.; Zakeeruddin, S. M.; Humphry-Baker, R.; Liska, P.; Charvet, R.; Comte, P.; Nazeeruddin, M. K.; Péchy, P.; Takata, M.; Miura, H.; Uchida, S.; Grätzel, M. *Adv. Mater.* **2006**, *18*, 1202−1205.
(34) Tsao, H. N.; Yi, C.; Moehl, T.; Yum, J.-H.; Zakeeruddin, S. M.; Nazeeruddin, M. K.; Grätzel, M. *ChemSusChem* **2011**, *4*, 591−594.
(35) Zeng, W. D.; Cao, Y. M.; Bai, Y.; Wang, Y. H.; Shi, Y. S.; Zhang, M.; Wang, F. F.; Pan, C. Y.; Wang, P. *Chem. Mater.* **2010**, *22*, 1915−1925.
(36) Lu, X.; Feng, Q.; Lan, T.; Zhou, G.; Wang, Z.-S. *Chem. Mater.* **2012**, *24*, 3179−3187.
(37) Cui, Y.; Wu, Y. Z.; Lu, X. F.; Zhang, X.; Zhou, G.; Miapeh, F. B.; Zhu, W. H.; Wang, Z. S. *Chem. Mater.* **2011**, *23*, 4394−4401.
(38) Zhu, W. H.; Wu, Y. Z.; Wang, S. T.; Li, W. Q.; Li, X.; Chen, J. A.; Wang, Z.-S.; Tian, H. *Adv. Funct. Mater.* **2011**, *21*, 756−763.
(39) Cai, L.; Tsao, H. N.; Zhang, W.; Wang, L.; Xue, Z.; Grätzel, M.; Liu, B. *Adv. Energy Mater.* **2013**, *3*, 200−205.
(40) Delcamp, J. H.; Yella, A.; Holcombe, T. W.; Nazeeruddin, M. K.; Grätzel, M. *Angew. Chem., Int. Ed.* **2013**, *52*, 376−380.
(41) Choi, H.; Kang, S. O.; Ko, J.; Gao, G.; Kang, H. S.; Kang, M. S.; Nazeeruddin, M. K.; Grätzel, M. *Angew. Chem., Int. Ed.* **2009**, *48*, 5938−5941.
(42) Jiang, K. J.; Masaki, N.; Xia, J. B.; Noda, S.; Yanagida, S. *Chem. Commun.* **2006**, 2460−2462.
(43) Chen, C. Y.; Wu, S. J.; Wu, C. G.; Chen, J. G.; Ho, K. C. *Angew. Chem. Int. Ed.* **2006**, *45*, 5822−5825.
(44) Gao, F. F.; Wang, Y.; Zhang, J.; Shi, D.; Wang, M. K.; Humphry-Baker, R.; Wang, P.; Zakeeruddin, S. M.; Grätzel, M. *Chem. Commun.* **2008**, 2635−2637.
(45) Kim, S.; Kim, D.; Choi, H.; Kang, M. S.; Song, K.; Kang, S. O.; Ko, J. *Chem. Commun.* **2008**, 4951−4953.
(46) Feng, Q.; Zhang, W.; Zhou, G.; Wang, Z.-S. *Chem. Asian J.* **2013**, *8*, 168−177.
(47) Chen, L. X.; Xiao, S.; Yu, L. *J. Phys. Chem. B* **2006**, *110*, 11730−11738.
(48) Wang, Z.-S.; Kawauchi, H.; Kashima, T.; Arakawa, H. *Coord. Chem. Rev.* **2004**, *248*, 1381−1389.
(49) Wang, H.; Feng, Q.; Gong, F.; Li, Y.; Zhou, G.; Wang, Z.-S. *J. Mater. Chem. A* **2013**, *1*, 97−104.
(50) Schlichthorl, G.; Huang, S. Y.; Sprague, J.; Frank, A. J. *J. Phys. Chem. B* **1997**, *101*, 8141−8155.
(51) Schlichthorl, G.; Park, N. G.; Frank, A. J. *J. Phys. Chem. B* **1999**, *103*, 782−791.
(52) Park, N. G.; Schlichthorl, G.; van de Lagemaat, J.; Cheong, H. M.; Mascarenhas, A.; Frank, A. J. *J. Phys. Chem. B* **1999**, *103*, 3308−3314.
(53) Kruger, J.; Plass, R.; Gratzel, M.; Cameron, P. J.; Peter, L. M. *J. Phys. Chem. B* **2003**, *107*, 7536−7539.
(54) Duffy, N. W.; Peter, L. M.; Rajapakse, R. M. G.; Wijayantha, K. G. U. *J. Phys. Chem. B* **2000**, *104*, 8916−8919.
(55) Schipper, D. J.; Fagnou, K. *Chem. Mater.* **2011**, *23*, 1594−1600.
(56) Wada, S.; Suzuki, H. *Tetrahedron Lett.* **2003**, *44*, 399−401.
(57) Masuda, N.; Tanba, S.; Sugie, A.; Monguchi, D.; Koumura, N.; Hara, K.; Mori, A. *Org. Lett.* **2009**, *11*, 2297−2300.
(58) Feng, Q.; Zhou, G.; Wang, Z.-S. *J. Power Sources* **2013**, *239*, 16−23.
(59) Chou, H.-H.; Chen, Y.-C.; Huang, H.-J.; Lee, T.-H.; Lin, J. T.; Tsai, C.; Chen, K. *J. Mater. Chem.* **2012**, *22*, 10929−10938.
(60) Kitamura, T.; Ikeda, M.; Shigaki, K.; Inoue, T.; Anderson, N. A.; Ai, X.; Lian, T.; Yanagida, S. *Chem. Mater.* **2004**, *16*, 1806−1812.
(61) Hara, K.; Wang, Z.-S.; Sato, T.; Furube, A.; Katoh, R.; Sugihara, H.; Dan-Oh, Y.; Kasada, C.; Shinpo, A.; Suga, S. *J. Phys. Chem. B* **2005**, *109*, 15476−15482.
(62) Hagberg, D. P.; Edvinsson, T.; Marinado, T.; Boschloo, G.; Hagfeldt, A.; Sun, L. C. *Chem. Commun.* **2006**, 2245−2247.
(63) Li, S.-L.; Jiang, K.-J.; Shao, K.-F.; Yang, L.-M. *Chem. Commun.* **2006**, 2792−2794.

(64) Hagfeldt, A.; Boschloo, G.; Sun, L.; Kloo, L.; Pettersson, H. *Chem. Rev.* **2010**, *110*, 6595−6663.
(65) Frisch, M. J.; Trucks, G. W.; Schlegel, H. B.; Scuseria, G. E.; Robb, M. A.; Cheeseman, J. R.; Montgomery, J. A.; Vreven, J. T.; Kudin, K. N.; Burant, J. C.; Millam, J. M.; Iyengar, S. S.; Tomasi, J.; Barone, V.; Mennucci, B.; Cossi, M.; Scalmani, G.; Rega, N.; Petersson, G. A.; Nakatsuji, H.; Hada, M.; Ehara, M.; Toyota, K.; Fukuda, R.; Hasegawa, J.; Ishida, M.; Nakajima, T.; Honda, Y.; Kitao, O.; Nakai, H.; Klene, M.; Li, X.; Knox, J. E.; Hratchian, H. P.; Cross, J. B.; Bakken, V.; Adamo, C.; Jaramillo, J.; Gomperts, R.; Stratmann, R. E.; Yazyev, O.; Austin, A. J.; Cammi, R.; Pomelli, C.; Ochterski, J. W.; Ayala, P. Y.; Morokuma, K.; Voth, G. A.; Salvador, P.; Dannenberg, J. J.; Zakrzewski, V. G.; Dapprich, S.; Daniels, A. D.; Strain, M. C.; Farkas, O.; Malick, D. K.; Rabuck, A. D.; Raghavachari, K.; Foresman, J. B.; Ortiz, J. V.; Cui, Q.; Baboul, A. G.; Clifford, S.; Cioslowski, J.; Stefanov, B. B.; Liu, G.; Liashenko, A.; Piskorz, P.; Komaromi, I.; Martin, R. L.; Fox, D. J.; Keith, T.; Al-Laham, M. A.; Peng, C. Y.; Nanayakkara, A.; Challacombe, M.; Gill, P. M. W.; Johnson, B.; Chen, W.; Wong, M. W.; Gonzalez, C.; Pople, J. A. *Gaussian03, Revision C.02*; Gaussian, Inc.: Wallingford, CT, 2004.
(66) Gregg, B. A.; Pichot, F.; Ferrere, S.; Fields, C. L. *J. Phys. Chem. B* **2001**, *105*, 1422−1429.
(67) Wu, J. H.; Lan, Z.; Lin, J. M.; Huang, M. L.; Hao, S. C.; Sato, T.; Yin, S. *Adv. Mater.* **2007**, *19*, 4006−4011.
(68) Wang, P.; Zakeeruddin, S. M.; Moser, J. E.; Nazeeruddin, M. K.; Sekiguchi, T.; Grätzel, M. *Nat. Mater.* **2003**, *2*, 402−407.
(69) Wang, P.; Zakeeruddin, S. M.; Exnar, I.; Grätzel, M. *Chem. Commun.* **2002**, 2972−2973.
(70) Neale, N. R.; Kopidakis, N.; van de Lagemaat, J.; Grätzel, M.; Frank, A. J. *J. Phys. Chem. B* **2005**, *109*, 23183−23189.
(71) Kopidakis, N.; Neale, N. R.; Frank, A. J. *J. Phys. Chem. B* **2006**, *110*, 12485−12489.
(72) Huang, S. Y.; Schlichthorl, G.; Nozik, A. J.; Grätzel, M.; Frank, A. J. *J. Phys. Chem. B* **1997**, *101*, 2576−2582.
(73) Kopidakis, N.; Schiff, E. A.; Park, N. G.; van de Lagemaat, J.; Frank, A. J. *J. Phys. Chem. B* **2000**, *104*, 3930−3936.
(74) van de Lagemaat, J.; Frank, A. J. *J. Phys. Chem. B* **2001**, *105*, 11194−11205.
(75) Cai, N.; Zhang, J.; Xu, M.; Zhang, M.; Wang, P. *Adv. Funct. Mater.* **2013**, *23*, 3539−3547.